

# Adaptation of Propagation Models to Improve the Coverage Range Prediction of LoRaWAN Technology at 915 MHz in an Urban Environment

Carlos René Suarez-Suarez, Diego F. Rueda, Luis Carlos Timaná-Eraso, and Jose Leon-Leon

**Abstract**—Long Range Wide Area Network (LoRaWAN) technology has established new concepts for long-range wireless communication, being widely used in the implementation of IoT solutions. Therefore, it is crucial to validate the coverage of the signal and to know the distance at which a LoRaWAN communication system can be connected. This document investigates LoRaWAN technology for cases based on urban environments, so it can be used as a guide for those projects that require predicting the connection distance range of a LoRaWAN link. In addition, it serves as a tool for the reader when it comes to predicting the coverage of Long-Range Wide Area Network (LoRaWAN) technology. Measurements were made in a LoRaWAN network deployed in urban environments, where RSSI measurements were made in the city of Bogotá D.C., Colombia. Experimentally RSSI values were compared with four different propagation models at a frequency of 915 MHz in urban environments. The contribution of this work is an adjustment to widely used prediction models, according to the recommendation of the International Telecommunications Union (ITU) ITU-R P.1546, which allows estimating coverage in scenarios with characteristics similar to Bogotá D.C. This allows to know with precision the coverage before implementing the LoRaWAN communications system at 915 MHz. The results of comparing field measurements with fitted propagation models show that the Okumura model is the best predictor of coverage with a minimum error rate.

**Keywords**—LoRaWAN; propagation models; Internet of Things; urban coverage; fitted models

## I. INTRODUCTION

LoRaWAN (Low Power Wide Area Network) is the most suitable technology for transferring small amounts of data over long distances [1]. Short- and medium-range data transmission is gaining importance in Internet of Things (IoT)-oriented applications, such as collecting data from sensors and sending signals to actuators [2]. A special application of LoRaWAN is agriculture, in which sensors are installed directly in the field and measure environmental data is sent to remote storage systems, where the data is analyzed for decision making, monitoring the crop growth and guarantee crop quality.

The planning and implementation of a LoRaWAN network requires a coverage analysis that allows identifying the connection area with a Gateway, therefore, the empirical propagation

This work was supported by the grant No. 000000000000618 financed from internal science fund of Catholic University of Colombia.

Carlos René Suarez-Suarez, Diego F. Rueda, Luis Carlos Timaná-Eraso, and Jose Leon-Leon are with Department of Electronics and Telecommunication Engineering, Catholic University of Colombia, Bogotá, Colombia (e-mail: crsuarez@ucatolica.edu.co, dfrueda@ucatolica.edu.co, lctimana@ucatolica.edu.co, jleon@ucatolica.edu.co).

models are used to determine the radio coverage of this type of networks [3]. Different authors describe the technical transmission conditions of the devices used in their solutions, but there are few articles that have presented solutions that explore the performance of LoRa equipment [4]–[7] (e.g. transmission distances, energy consumption, reliability, packet collision, transmission security etc.). Additionally, there are studies in which empirical propagation models and experimental measurements are compared under certain field conditions [3], [8]. These articles compare the results of mathematical models with data from transmission tests received from prototypes, which measure environmental variables in urban crops located in densely populated areas. Existing mathematical models approved by the ITU such as Okumura-Hata, COST-231 Hata and ITU-R are evaluated [8], [9]. These studies focus on networks implemented with LoRa technology.

Although there are studies comparing experimental measurements and the predictions of propagation coverage models recognized by the ITU (International Union of Telecommunications) [8], [10]–[12], there is a lack of a detailed description of the calculation procedure in the literature, especially the calculation of the network communication link and the reachable transmission distance, taking into account the transmission parameters of the Gateways and LoRaWAN devices. For this reason, the objective of this document is to formulate a guide for the range prediction of LoRaWAN links.

In this way, the contribution of this document is to specify a methodology for predicting the propagation of radio waves based on LoRaWAN technology at 915 MHz and adjust the parameters of empirical ITU propagation models. The Received Signal Strength Indicator (RSSI) is obtained experimentally from a real implementation of a LoRaWAN link in an urban environment of the city of Bogotá D.C., Colombia. This indicator is compared with the values calculated from propagation models, so this work aims to provide a tool for adapting the mathematical equation of the empirical ITU propagation models and predicting the coverage of LoRaWAN technology for data transmission at a frequency of 915 MHz. Thus, identifying and fitting a propagation model that presents the lowest error rate, the coverage can be predicted with more accuracy before implementing the communications network for IoT applications in urban environments with similar characteristics that the city studied.

The document is organized as follows: Section II presents a review of previous studies, Section III details the empirical



propagation models, Section IV proposes a methodology to determine the coverage of the LoRaWAN network, Section V describes the materials and methods used to implement the tested LoRaWAN network and to perform the field measurements. The results of experimental measurements and fitted models as well as the comparison between measured values and those calculated by the empirical propagation models are presented in Section VI. The results are discussed in Section VII. Finally, the conclusions are presented in Section VIII.

## II. PREVIOUS WORKS

In the reviewed literature, a comparison between the measurements made in the field and the predictions of the empirical propagation coverage models recognized by the ITU (International Union of Telecommunications) for LoRaWAN networks is carried out in [8], [10]–[12]. These documents show experiments and analysis of results, in which the application of propagation models is tested in the design, planning and management of wireless networks, based on LoRa technology for different configurations. In [13], experiments were performed to measure the RSSI and the signal-to-noise ratio (SNR) with a LoRa transceiver for different solutions at a frequency of 915 MHz. In [14], it is presented the coverage of a LoRaWAN network in the 915 MHz frequency band for densely populated urban areas with communication protocols used in the Internet of Things (IoT). Data collection was performed in the city of Montreal to test coverage on highways in the downtown area [14]. On the other hand, other works were found such as [15]–[17] that focused on empirical tests in urban areas using LoRaWAN technology as well as efforts in the analysis of coverage gaps for areas with a dense urban infrastructure (as indicated in [4]). However, these investigations focused on the comparison of LoRaWAN coverage at different data rates in urban environments.

Meanwhile, in [18]–[20]) were analyzed LoRaWAN networks that operate on the 433, 865 and 915 MHz frequencies. Specifically, the coverage, capacity and performance rate of the final device were measured comparing different LoRa nodes and taking into account their performance in terms of signal strength and power requirements. In addition, the configuration of LoRa nodes parameters that were modified to find the best possible solution to transmit data over longer distances with the least loss of data packets is proposed. Finally, they performed measurements on a LoRaWAN network to characterize the spatial and temporal properties of the LoRaWAN channel at a distance from the nearest gateway of 7.5 km with an information loss of up to 70%.

In relevant works such as [21], [22], it is studied LoRa-based low-cost IoT network systems with open source components and software like gateways, end devices and a variety of sensors, which are used to characterize the performance of a LoRa network at the 915 MHz ISM Band indoors and outdoors. The results show that, i) when the gateway is located inside a concrete building, the network is able to achieve connection; the interior coverage is sufficient to cover a structure of a seven-story building with a minimum loss of packets transmitted, ii) outdoor coverage is highly dependent on the environment; in experiments, a communication range of 4.4 km was achieved with 15% loss of packets transmitted,

iii) network parameters such as dispersion factor and package size affects coverage; it has been found that a payload size of 242 bytes results in a 90% loss of transmitted packets compared to less than 5% loss of transmitted packets if the packet payload size is 1 byte. LoRaWAN technology presents a low-cost, high-performance multi-channel gateway. To validate the performance of the Gateway, its configuration consisted of a Raspberry Pi 3B+ and an iC880A LoRa hub as a gateway, the system was integrated with a 2.2 dBi omnidirectional antenna, with a maximum communication distance of 2.5 km and 1.3 km, in rural and urban areas respectively and a PER (Packet Error Rate) of less than 20%.

In [23], [24], technical solutions and measurement procedures were presented with a low-cost open source code to determine the coverage of a LoRaWAN network in dense urban environments, the quality of the transmission link is measured through a test methodology that calculates the network coverage. The results showed an average coverage range between 7 and 10 km to reach the connection with the gateway, likewise, ideas for planning and validating IoT networks based on LoRaWAN were proposed. The investigation analyzes the Pearson correlations generated from the measured value of RSSI between LoRaWAN nodes and a gateway with different parameters of the dispersion factor and test locations. From the tests performed, the resulting average Pearson correlations for indoor and outdoor measurements were about 0.2 and 0.3 to 0.4 respectively. It was also taken into account the 5-second interval between pings, reducing the average error by up to half during outdoor tests in sites with line of sight between LoRa equipment.

Table I presents a comparative summary of the previous works that were reviewed as part of the state of the art. According to the documents mentioned in this section, some working groups carry out tests and measurements with real equipment, others build tools to model the results and compare them with real tests. However, in the reviewed literature, the adaptation of the mathematical equation of the propagation models to predict the coverage of a LoRaWAN network was not found. Therefore, this work provides an original methodology for a more accurate prediction of the coverage range.

## III. EMPIRICAL MODELS OF POINT-TO-AREA PROPAGATION

According to recommendation ITU-R P.1546, which defines point-to-area propagation prediction methods for terrestrial wireless services in the frequency range from 30 to 4000 MHz [26], it is recommended to compare field measurements with the results obtained in the simulation tool for different models. Table II presents well-known general empirical propagation models such as Okumura [27], Okumura-Hata [28], Hata Cost [29] and other models, such as Walfish-Ikegami [30], [31] or Longley- Rice [32]. Subjective analyzes can decide which model is the best to model the field intensity in the VHF radio band that provide reasonably accurate predictions of coverage in land mobile radio systems and magnitude of the field strength in the coverage areas of radio stations. These models do not require complex calculations or detailed knowledge about particular propagation paths, therefore they can to be

TABLE I  
COMPARATIVE SUMMARY OF RELEVANT PREVIOUS WORKS

Author/Worked	Measurement city	Environment	Measured indicators	Studied models
Dobrilović et al. [11]	Zrenjanin, Serbia	Urban	Tx Power 18 dBm RSSI to -129 dBm Urban reaches 5 km Frequency 868 MHz	Lee propagation model
Chall, et al. [8]	Beirut city and Bekaa valley, Lebanon	Urban and rural	Tx Power 14 dBm RSSI to -120 dBm Rural reaches 9 km Rural reaches 10 km Frequency 868 MHz	Okumura-Hata model, ITU R, COST 231, 3GPP, Free Space
Ingabire et al. [12]	Glasgow, Scotland	Urban	Tx Power 14 dBm RSSI to -150 dBm Urban Reaches 2,5 km Frequency 868 MHz	ITU R 225 Extended Hata COST-231 Hata, Okumura-Hata
Nashiruddin et al. [25]	Kota Animalia	Suburban	Tx Power 16 dBm RSSI to -137 dBm Urban Reaches 11,6 km Frequency 923-925 MHz	Hata
Petajajarvi, et al. [4]	Oulu, Finland	Urban	Tx Power 14 dBm Urban Reaches 15 km Water 30 km Frequency 868 MHz	Channel attenuation mode
Alset, et al. [19]	Beirut city, and Bekaa valley	Rural and Urbam	Tx Power 16 dBm to 20 dBm RSSI to -137 dBm Urban reaches 10 km Frequencies 433, 865 and 915 MHz	Cost 231

used without high-resolution terrain data-bases. Most of the empirical propagation prediction models can be represented by a basic expression shown in equation (1) [27]:

$$P_R = P_T + G_T + G_R - L_{ST} - L_{SR} - L \quad (1)$$

where  $P_R$  is the power at the transmitter output, in logarithmic scale;  $G_T$  is the gain of the transmitting antenna;  $G_R$  is the gain of the receiving antenna;  $L_{ST}$  is the system losses at the transmitter, e.g., cable losses, connectors losses;  $L_{SR}$  are system losses at the receiver and  $L$  is the modeled propagation loss.

In the following subsections, it will be presented a synthetic description of the applications and mathematical concepts of the models: Okumura [27], Okumura-Hata [28] Hata Cost [29], Walfish-Ikegami [30]–[32] and Longley-Rice [33].

#### A. Okumura Model

The mathematical model determines the power loss of the transmitted signal. First the path loss in free space between transmitter and receiver is determined, then the value of  $A_{mu}(f, d)$  is added together with correction factors to take into account the type of terrain. The model can be expressed as

$$L_{50} \text{ dB} = L_F + A_{mu}(f, d) - G_{hte} - G_{hre} - G_{Area} \quad (2)$$

where  $L_{50}$  is the 50<sup>th</sup> percentile of the value of the propagation path loss,  $L_F$  is the free space propagation loss,  $A_{mu}$  is the median attenuation relative to free space,  $G_{hte}$  is the gain factor of the base station antenna height,  $G_{hre}$  is the mobile antenna height gain factor and  $G_{Area}$  is the gain due

to the type of environment. Antenna height gains are strictly a function of height and have nothing to do with antenna patterns.

#### B. Hata-Cost Model

There are two versions of the Okumura Hata model, the first exposes the loss of power of the transmitted signal, it is expressed according to

$$P_L = PL_{EL} + A_{exc} + H_{cb} + H_{cm} \quad (3)$$

where  $PL_{EL}$  is the direct path free space loss;  $A_{exc}$  is the excess path loss for a transmitting antenna height of 200 meters and a receiving antenna height of 3 meters;  $H_{cb}$  and  $H_{cm}$  are both a correction factors. The standard formula for path loss is expressed as

$$P_L = A + B * \log(R) + C \quad (4)$$

where  $A$ ,  $B$  and  $C$  are factors that depend on both the frequency and the antenna height as follows:

$$A = 69.55 + 26.16 * \log(f) - 13.82 * \log(h_{bs}) - a(h_{ms}) \quad (5)$$

$$B = 44.9 - 6.55 * \log(h_{bs}) \quad (6)$$

where  $f$  is the frequency in MHz,  $R$  is the distance in km,  $h_{bs}$  is the transmitting antenna height,  $a(h_{ms})$  is a function of the receiving antenna height  $h_{ms}$  and the factor  $C$  depends on the environment as shown in (10):

TABLE II  
 CHARACTERIZATION OF PROPAGATION MODELS

Propagation Model	Description
Okumura-Hata	It is used in the planning of land mobile services, in a wide variety of terrain with obstacles such as vegetation, buildings in urban areas for different wavebands centered on 150, 450, 900 and 1500 MHz, based on typical propagation conditions in and around Tokyo, Japan [27]. It is a simplified version of the Okumura model (also called the Okumura-Hata model) and provides mathematical formulas that approximate the Okumura model for a frequency range between 100 to 1500 MHz, distances from the transmitter site between 1 to 20 km and heights of the transmitting antennas between 30 to 200 m above the surrounding terrain [28].
Hata-Cost	This model is derived from a model proposed by Hata, created to be used in macrocells for frequency bands higher than 1500 MHz. It is valid for transmission antennas located between 30 m and 200 m, and receiver antennas from 1 to 10 m [29].
Walfisch-Ikegami	It is a precise statistical description of an urban environment [30], valid for mobile station (MS) heights between 1 m and 3 m and Base Station (BS) antenna heights between 4 and 50 m high [31]. In addition, it is considered for a range from 800 MHz to 2000 MHz, and includes links without and with line of sight.
Longley-Rice	It is a radio wave propagation prediction model used for the frequency range from 20 MHz to 20 GHz, in areas with various climatic and terrain conditions and a distance ranging between 1 and 2000 km [32].

$$L_b = 46.3 + 33.9 * \log\left(\frac{h_{bs}}{m}\right) - a(h_{ms}, f) + \left(44.9 - 6.55 * \log\left(\frac{h_{bs}}{m}\right)\right) * \log\left(\frac{R}{km}\right) + C \quad (7)$$

where  $L_b$  is the median path loss;  $f$  is the transmission frequency;  $h_{bs}$  is the transmitting antenna height;  $R$  the link distance;  $h_{ms}$  is the receiving antenna height;  $a(h_{ms})$  is the receiving antenna height correction factor as described in the Hata model for urban areas. For suburban or rural settings,  $a(h_{ms}, f)$  factor is defined using the equation (8):

$$a(h_{ms}, f) = \left(1.1 * \log\left(\frac{f}{MHz}\right)\right) * \frac{h_{ms}}{m} - \left(1.56 * \log\left(\frac{f}{MHz}\right) - 0.8\right) \quad (8)$$

For urban settings (i.e. large cities) it is calculated by the equation (9):

$$a(h_{ms}, f) = \begin{cases} 8.29 * (\log(1.54h_{ms}))^2 - 1.1, & \text{if } 150 \leq f \leq 200 \\ 3.2 * (\log(11.75h_{ms}))^2 - 4.97, & \text{if } 200 \leq f \leq 1500 \end{cases} \quad (9)$$

Finally, a constant offset  $C$  is applied as shown in the equation (10):

$$C = \begin{cases} 0 \text{ dB} & \text{for medium-sized or suburban cities} \\ 3 \text{ dB} & \text{for metropolitan areas} \end{cases} \quad (10)$$

### C. Longley-Rice Model

It is a widely accepted model in industry as well as by the Federal Communications Commission (FCC). This model was initially developed for the frequency planning of TV broadcasting in the US. This model allows predictions in an area and forecasts of point-to-point links. Some parameters that are required for this propagation model are: frequency, whose nominal range is between 20 MHz and 20 GHz; Effective Radiated Power (ERP); transmitter antenna operation, which is assumed to be omnidirectional if the directional antenna is not specified; height of the antenna above the ground (meters or feet) which is defined manually; effective height for the calculations is estimated by the model itself; antenna polarization (vertical or horizontal); refractivity of the atmosphere, measured in N parts per million, which typically ranges from 250 to 400 N units; 4/3 effective earth curvature corresponds to a surface refractivity of 301 N units, and Longley-Rice recommends 301 N units for average atmospheric conditions. The surface refractivity  $N_s$  from the effective earth curvature  $K$  is given by

$$N_s = 179.3 * \ln\left[\frac{1}{0.04665} \left(1 - \frac{1}{K}\right)\right] \quad (11)$$

Other parameters that are considered by the model are the permittivity, which is the dielectric constant of the soil; soil conductivity; climatic zone defined according to climatic codes; situation variability expressed as a percentage where a variability of 50% is considered normal for coverage estimates; and time variability which is also expressed as a percentage (from 0% to 100%). The Longley-Rice model uses elevation values to create a brief profile of a route for program analysis. These elevation values are taken from the Terrain Analysis Package (TAP) database. The original model uses the same increments along a terrain profile specified path.

### D. COST-231 Walfisch-Ikegami Model

This model is considered by the ITU-R in the IMT-2000 recommendations. This model combines some empirical correction parameters with the parameters of path loss from the Walfisch-Bertoni model and path loss in a building from the Ikegami model. The model is restricted to flat urban terrain and in the complex Fresnel equation it is possible to relate the distances between the two ends of the path and the top of the obstacle. Also, it also allows to determine the path power loss in dB which is given by

$$PL(dB) = L_o + L_{rts} + L_{msd} \text{ for NLOS} \quad (12)$$

where,  $L_o$  is the free space loss,  $L_{rts}$  is the roof-to-street diffraction and scattering loss, and  $L_{msd}$  is the multiscreen diffraction. Each of these losses is given by the equations (13), (14) and (15), respectively:

$$L_o = 32.4 + 20 * \log(R) + 20 * \log(f) \quad (13)$$

$$L_{rts} = -8.2 + 20 * \log(a) + 20 * \log(H) + L_{ori} \quad (14)$$

$$L_{msd} = L_{bsh} + K_a + K_d * \log(R) + K_f * \log(f) - 9 * \log(b) \quad (15)$$

where,  $R$  is the distance link;  $a$  is the street width;  $H$  is the antenna average height,  $L_{ori}$  is a correction factor, which are found taking into account the angle  $\alpha$  proposed in the original model and it is governed under certain conditions;  $h_b = h_{eb}$  is the receiving antenna height, and  $h_r = h$  is the buildings height.

#### IV. PROPOSED METHODOLOGY TO SELECT AND TUNE THE PROPAGATION MODEL

The methodology proposed in this paper allows to select and tune a propagation model from measured values in a real context and estimates values from a empirical propagation model. A comparison and analysis is carried out between measured and calculated values. Finally, the equations parameters of the mathematical models are fitted and the one that provides the closest results to the measurements is chosen. Each of the steps included in the process contained in this methodology is shown in Fig. 1

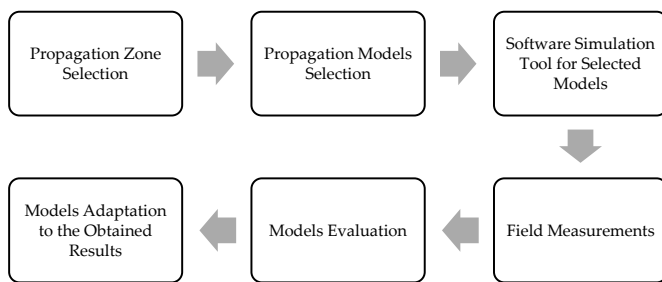


Fig. 1. Step-by-step of the proposed procedure

##### A. Propagation Zone Selection

According to [27], it is important to ensure that this coverage area has been chosen for the tests in such a way that it represents the most typical propagation conditions of the region (urban/suburban, vegetation density, terrain irregularities, etc.). Due to the conditions of the project, the central sector of the city of Bogotá has been selected. The recommendation is to measure the received power in a node along the available radial route (for example, a highway), within the coverage area and at points located at given intervals, for example, 1 km. One of the possible assemblies to carry out these measurements is shown in Fig. 2

##### B. Propagation Models Selection

Before applying a general empirical model in a given region with unknown characteristics, it is advisable to test the performance of the selected model or compare the performance of various models [27]. The models described in Table II are considered, the mathematical calculations are performed, and finally, the received RSSI is recorded in a table for a given distance from the transmitter.

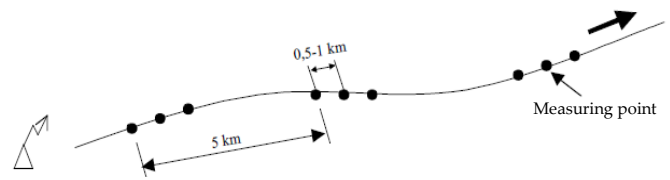


Fig. 2. Test model according to ITU recommendation [29]

##### C. Software Simulation Tool for Selected Models

In this phase, the selected models are implemented in a software simulation tool. For modeling, software tools can be built using spreadsheets or scripts, a simple Matlab script or any mathematical software, including Excel. Additionally, it can be simulated using specialized software with which the coverage area can be theoretically predicted for the communications system they may have. There is free distribution software such as Radio Mobile for calculating long-distance radio links on irregular terrain. Likewise, there are different licensed software tools on the market that use geographic profiles with equipment information (power, receiver sensitivity, antenna characteristics, losses, etc.) such as Xirio or RadioMobile.

##### D. Field Measurements

Measurements can be done fairly quickly and with very little human and financial resources. For a more formal and descriptive explanation of the measurement process, it is recommended to refer to the ITU Spectrum Monitoring Manual [33]. The recommendation proposed in [26] is described below. The first step is the selection of the test (reference) transmitter and receiver. It is advisable to use existing transmitters in the area of interest.

The points to carry out the RSSI measurements of the propagation zone link are defined. Then, the more measurements are carried out, the better the results will be. To perform a test it is enough to carry out static ground measurements in coverage areas of at least two or three existing radio transmitters. In each of the selected coverage areas, it is convenient to make ground measurements with at least 15 or 20 different distances from the transmitter. For each of these distances, the measurement sample should include at least 5 or 10 measurements, preferably taken in different directions from the transmitter, to ensure the correct assessment of the median field strength. If the transmitters used in the test have directional antennas, the measurement points must all be within the main beam of the transmitter antenna. The test receiver antenna will be mounted at an appropriate height, which for the purposes of this project is 1.5 to 2m.

Once the equipment has been selected, it is convenient to draw a plan to make the measurements. For this, an appropriate scale map can be used, in which the measurement routes will be traced as well as the measurement points for the static measurements. Static measurements are performed in this study. Normally in a LoRaWAN network the gateway is equipped with the necessary automated measurement functions. Typically, measurements are taken at least 15 to 20 points, equally spaced throughout the coverage area.

### E. Models Evaluation

The measurement results are recorded in a table as a function of the distance from the test transmitter. This also allows immediate comparison of the average measured values of the field strength with the results obtained by one or more propagation models. Conventional computer programs, spreadsheets and Radio Mobile software can be used to automate this exercise.

The results obtained from the theoretical models selected in subsection IV-B are compared with the RSSI measured in subsection IV-D. So that a pattern is established in each of the models and then the prediction of each of the models is determined. Finally, the mean square error is established with the measurement made with the LoRaWAN equipment at a frequency of 915 MHz.

### F. Models Adaptation to the Obtained Results

The results of the measured values are compared with the calculated values. Trend graphs are built and the existing equations are adjusted. So that two basic empirical parameters appear: slope  $\gamma$  and initial deviation  $K$ . The model adjustment process consists of modifying those two parameters of equation 16 to the equations of the mathematical models described in Section III using the least squares criterion.

$$E_R = -\gamma * \log(R) + K (P_{bs}, f, h_{bs}, h_{ms}, \dots) \quad (16)$$

## V. MATERIALS AND METHODS

In this section are described the LoRaWAN network equipment used in the deployment of a LoRaWAN network to perform field measurements. Additionally, the configuration parameter of the network are presented. Finally, the way the tests were performed is described.

### A. Test Network Topology

A sensor system is implemented, in which environmental variables are measured and sent to a LoRaWAN gateway interconnected to a server by means of a microprocessor-transmitter system. Fig. 3 shows the implemented LoRaWAN topology for testing.

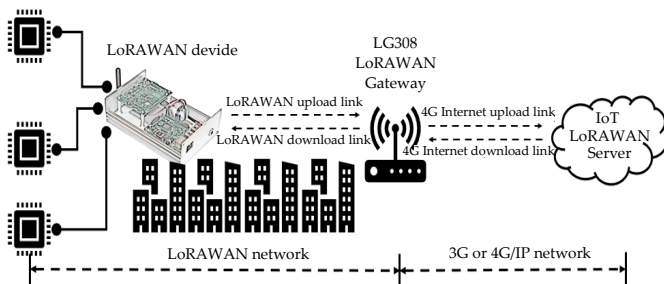


Fig. 3. Implemented scenario for testing a LoRaWAN network

1) *LoRaWAN Nodes*: As final devices in measurements, we have used LoRaMote, which is equipped with a Semtech SX1272 transceiver connected with a 5 dBi omnidirectional antenna. A system of sensors that measure environmental variables connected by cable to a Raspberry Pi 4B card has been implemented, which in turn is connected to a 915 MHz LoRaWAN transmission card. The firmware version programmed for the node was 3.1. In addition to the SX1272 transceiver, each node included a GPS (Global Positioning System) receiver and sensor array. During the measurements, the nodes were powered by 5 V batteries at approximately 2 m in height from the ground, see Fig. 4.

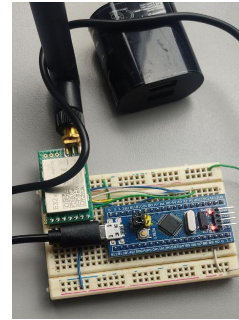


Fig. 4. LoRaWAN Node implemented

2) *LoRaWAN Gateway*: An LG308 LoRaWAN Gateway was used to interconnect the LoRaWAN wireless network to an IP network through WiFi, Ethernet, 3G or 4G mobile network. The mobile network can be used as a main connection to the Internet or as a backup. The gateway was located on the third floor of the Catholic University's building with an omnidirectional antenna. The antenna is 12 m above the ground and provides a gain of 9 dBi over the 915 MHz band. The LoRaWAN gateway used in the test scenario is shown in Fig. 5.



Fig. 5. LoRaWAN Node implemented

3) *LoRaWAN Server*: A global collaborative IoT ecosystem was implemented, which manages networks, devices, and solutions using LoRaWAN®. It provides a global open network and toolset to build IoT applications at low cost, with maximum security, and ready to scale.

### B. LoRa WAN Frequency Band

The LoRaWAN communication operates without a license in several frequency bands based on the specifications of the regional parameters document [34], which contains a summary of the radio regulations. Table III presents a summary of the LoRaWAN frequency plans [25].

TABLE III  
LoRaWAN FREQUENCIES

LoRaWAN Frequency Plan	Name
EU 863-870 MHz ISM Band	EU868
US 902-928 MHz ISM	US915
CN 779-787 MHz ISM Band	CN779
EU 433 MHz ISM Band	EU433
AU 915-928 MHz ISM Band	AU915
CN 470-510 MHz ISM Band	CN470
AS 923 MHz ISM Band	AS923
KR 920-923 ISM Band	KR920
IN 865-867 ISM Band	IN865
RU 864-870 ISM Band	RU864

### C. Tests Configuration

The field measurements were carried out in the city of Bogotá, Colombia, in October 2022 under different climatic conditions. The population of Bogotá is approximately 8,000,000 inhabitants, and the tallest residential buildings identified in the measurement zone are between 12 and 20 stories high. There are no major differences in geographic elevation, so the landform is mostly flat. The zone presents highly dense vehicular traffic. During all the measurements, the gateway was conditioned in an interior space, while the final LoRaWAN device was operating outdoors. The transmission consisted of sending information units of the constant size of 40 Bytes from LoRaWAN device to the gateway. Each information unit included a sequence number and GPS coordinates, which were used to estimate the packet loss rate and the position of the transmitting node, respectively. During the measurements, both gateway and devices remained static.

The RSSI value [19] (in dBm) was used to measure the power (in mW) of the signal at the receiver, and this can indicate the number of data packets received. The RSSI is generally measured in negative numbers and a value that is closer to zero is generally considered a better signal. Typically, the RSSI value of LoRa SX1276 ranges from -148 dBm to 0 dBm. Receiver sensitivity is calculated using the equation (17), which is important in LoRaWAN end node selection:

$$S = -174 + 10 * \log(BW) + NF + SNR_{limit} \quad (17)$$

where,  $S$  is the receiver sensitivity in dBm;  $BW$  is the frequency bandwidth which was 125 kHz (default);  $NF$  is the noise figure in dB and depends on the hardware implementation, e.g. LoRaWAN end node transceiver chips like SX1276 and SX1278 operate under  $NF = 6$  dB; and  $SNR_{limit}$  is the signal to noise ratio of -20 dB which indicates how strong the signal has to be compared to the noise and is related to  $SF$  (Spread Factor). Based on equation (1), the change in sensitivity due to selection is tabulated in Table IV for different  $SF$  values and their corresponding  $SNR$  values.

Table IV shows that as the  $SF$  increases, the sensitivity values also increase. Furthermore, the signal becomes weaker as the distance between the device and the LoRaWAN gateway increases. In such circumstances, the  $SF$  value is increased

TABLE IV  
CALCULATED VALUES OF RECEIVING SENSITIVITY AS A FUNCTION OF SF VALUES

SF	BW (kHz)	NF (dB)	$SNR_{limit}$ (dB)	Sensitivity (dBm)
7	125	6	-7.5	-1.25
8	125	6	-10	-1.27
9	125	6	-12.5	-1.30
10	125	6	-15	-1.32
11	125	6	-17.5	-1.35
12	125	6	-20	-1.37

to improve the receiver demodulation sensitivity. Therefore,  $SF = 7$  typically means that the device is very close to the gateway, while  $SF = 12$  means that the device is far from the gateway with respect to the  $SNR$  limits.

Since the objective of the measurements was to find the maximum communication range, the devices were configured to use the largest possible spread factor, that is,  $SF = 12$ . This resulted in low data rate, but improved the base station sensitivity to -137 dBm. LoRaWAN signal bandwidth is set to 125 kHz

In each of the measurement points, the received RSSI intensity values were recorded one by one. Through descriptive statistics strategies, the median field intensity was obtained as a function of the distance from the transmitter. The distances with respect to the transmitter were determined from the geographical coordinates, i.e., a GPS receiver that allowed to measure differences in distance, the vehicle odometer or a map at the appropriate scale.

## VI. RESULTS

In this section is presented the propagation models calculation and the field measurements obtained in each experimental scenario. A data analysis is also carried out to compare the theoretical and experimental values of losses and RSSI. Finally, a model adjustment is performed by fine-tuning its empirical parameters.

### A. Propagation Models Calculation and Field Measurements

The measurements made in the LoRaWAN test network made it possible to obtain a set of field strength values for given distances, in which signal reception experiments were carried out with an end LoRaWAN device developed by the authors as well as using the RSSI measurement with a spectrum analyzer. These measurements can be compared with the modeling results, emphasizing the adjustment of the model parameters (antenna height, radiated power, etc.) for each of the measurement routes. Table V shows the results obtained for field intensity with an effective radiated power (ERP) of -11 dB, receiving antenna height of 2 m, transmitting antenna height of 8 m, buildings height of 20 m, and street width of 13 m. Note that the field intensity is calculated from the theoretical and measured RSSI values.

During the data collection experimentation, a series of three routes were chosen in different sectors of Bogotá, called Direction Route (DR) from DR0 to DR2. Experiment 1 was

TABLE V  
 RECORD OF MEASUREMENTS, IN WHICH THE RESULTS OF MODELING AND MEASUREMENTS ARE COMPARED

Free space loss (dB)	Points (km)	Modeling results (dB $\mu\text{V/m}$ )								Experimental results									
		Okumura	Hata Cost	Longley-Rice	COST 231-Walfisch Ikegami	Real (dB $\mu\text{V/m}$ )	Deviation	Quantity	Reliability (+/- dB)	Measures (dB $\mu\text{V/m}$ )									
										R1	R2	R3	R4	R5	R6	R7	R8	R9	R10
89.63	0.1	94.64	102.93	78.3	90.52	132.1	3.07	10	-1.000	132	135	129	129	134	136	135	134	129	128
90.23	0.2	100.66	115.86	85.1	105.63	148.1	4.61	10	-0.699	151	148	147	142	150	142	144	156	148	153
90.58	0.3	104.18	123.42	87.8	114.47	149.7	3.71	10	-0.523	156	150	151	150	147	142	151	147	151	152
90.83	0.4	106.68	128.78	92.2	120.74	148.6	1.96	10	-0.398	151	148	147	150	145	147	150	151	148	149
91.03	0.5	108.62	132.94	99.5	125.60	146.7	3.20	10	-0.301	144	145	143	143	144	151	149	150	150	148
91.18	0.6	110.20	136.34	98.1	129.58	147.3	3.68	10	-0.222	144	146	147	141	143	151	151	149	150	151
91.32	0.7	111.54	139.21	98.7	132.94	150.6	1.96	10	-0.155	148	151	151	153	148	153	152	152	149	149
91.43	0.8	112.70	141.70	99.9	135.85	147.7	4.35	10	-0.097	148	151	151	142	148	154	148	139	148	148
91.54	0.9	113.72	143.90	99.5	138.42	151.6	1.17	10	-0.046	151	150	150	152	151	153	151	153	153	152
91.63	1	114.64	145.86	101.6	140.66	150.5	1.58	10	0.000	153	150	152	150	151	148	151	151	151	148

focused on sector DR0, while sectors DR1 and DR2 were part of experiment 2. As part of the route selection, the most complete degree of coverage possible was obtained for streets in and around the Catholic University of Colombia. Fig. 6 shows the tracks (in black) followed during data collection, and represents the routes followed. The circles indicate the following distances from the LoRaWAN Gateway: 0.1 km, 0.2 km, 0.3 km to 1 km, so the longest distance traveled from the LoRa Gateway was about 1 km. However, most of the tests were performed within a 1 km radius from the LoRaWAN Gateway. Regarding the elements to calculate the equipment link, the the mobile transmitter power and the Gateway receiver sensitivity were  $P_{TX} = 16.9$  dBm and  $P_{RX} = -137$  dBm, respectively.

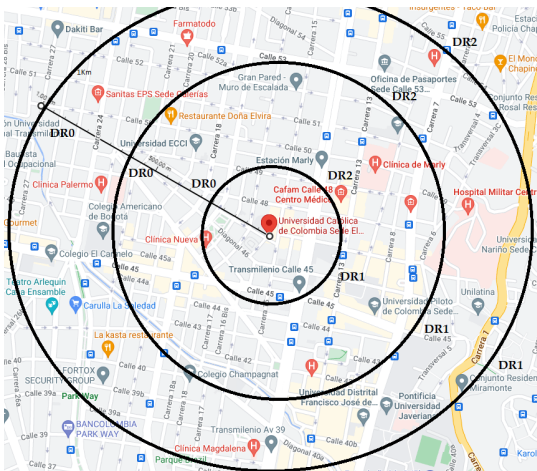


Fig. 6. Test model according to ITU recommendation

### B. Data Analysis and Comparison

In our measurements, the implemented LoRaWAN network was configured with a bandwidth of 125 kHz, a few units of information were received and it was decided to propose the attenuation model for a particular channel at a frequency of 915 MHz. The proposed model can be used to briefly estimate the communication distance for LoRaWAN technology in similar areas. The measured received signal strength (RSSI) was used to calculate the path loss (PL) using the equation (18):

$$PL = |RSSI| + SNR + P_{TX} + G_{RX} \quad (18)$$

The standard deviation (std) of signal fading (SF) describes a deviation between the measured  $PL$  and the expected  $EPL$  and is given by the equation (19):

$$\sigma_{SF} = std(PL - EPL) \quad (19)$$

Path loss calculations and experimental measurements were performed at the points described in subsection VI-A. After the measurements were made in various coverage areas, those that best fit the model were selected using the least squares criterion:

$$\sum_{i=1}^n [y'_i - \gamma(x_i, a, b, c, \dots)]^2 = \min \quad (20)$$

where,  $y'_i$  is the experimental result at point  $x_i$ ;  $n$  is the number of measurements in a route; and  $\gamma(x_i, a, b, c, \dots)$  is the result of the model for point  $x_i$  and transmitter parameters  $a, b, c$ . Fig. 7 shows the result of the path losses, which is a comparison of values obtained theoretically from the models studied with the measured values. Fig. 8 shows the RSSI calculated and measured for each model.

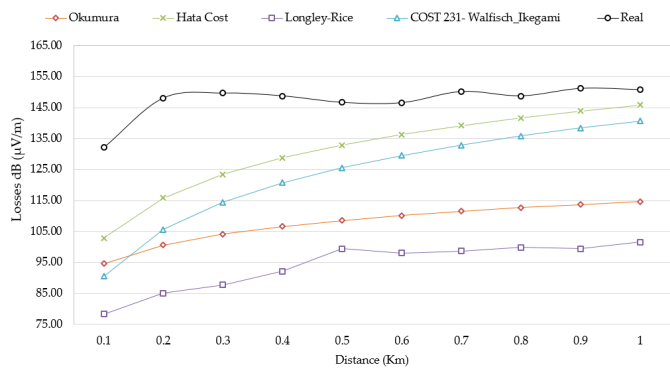


Fig. 7. Calculated losses for propagation models using default parameters and measured values

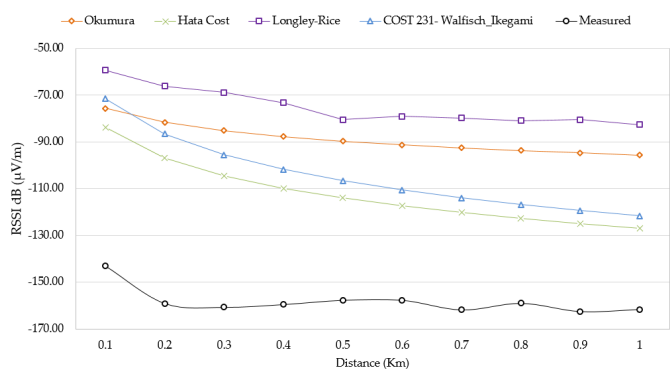


Fig. 8. Calculated RSSI for propagation models using default parameters and measured values

According to the LG308 LoRaWAN Gateway specifications, the range was predicted with an RSSI=-137dBm, which was obtained with the calculations from equation 17 and the data in Table IV. It follows that with the Okumura and Longley-Rice models it would have a range greater than 20 km, from the Hata Cost and COST 231-Walfisch-Ikegami models, a range of 1.6 and 1.9 km were obtained, respectively. However, in the measurements made in the field, a range smaller was achieved, so the adjustment to the equations of the mathematical models presented was made.

The performance of models can be evaluated more formally and they can be compared with each other through the application of statistical measurements and analyses, such as the least squares criterion. According to this criterion, the model that best fits the results obtained experimentally will yield a minimum in equation (20). It is clear, that if  $\gamma(x_i, a, b, c, \dots)$  is substituted by various tested models, then the results of equation (20) can be calculated.

For all series of experimental measurements, the unbiased performance of each of the tested models can be evaluated in all cases, by combining all these comparisons. The most appropriate model can be chosen because it is the one that provides the best fit with the experimental results. In Table VI, the values calculated from equation (20) were recorded in the error column. When comparing the registered data of the models with the registered data of the measurements carried out and noted in Table VI.

Table VI shows the measured and calculated trajectory losses in dB for each model, as well as the calculated and measured RSSI. For the measured case, the path loss is higher, it can be caused by buildings and other obstacles blocking the path between the end device or node and the gateway.

When the device presented a free path in the transmission to the gateway, the path loss was greater than 53 dB above the Longley-Rice model, 40 dB above the Okumura model, 23 dB above the Walfisch Ikegami model and 16 dB above the Hata Cost model. It was possible to select the results of the measurements that best fit the model using the least squares criterion. These results show that the Hata-Cost model provides the best approximation with an average error of 0.2932 between theoretical and measured losses.

### C. Model Adaptation

Since the tests showed that the precision of the empirical model found in subsection VI-B is not sufficient, it is considered necessary to adjust the model. This can be done by fine-tuning its empirical parameters. The different equations were taken and the pattern to be modified in the equations is established according to the error presented in Table VI. Calculations are made again with that adaptation and it is determined which model has the best results and the measured values are comparable with the calculated values as seen in Table VII.

The accuracy of the selected general empirical model with respect to particular propagation conditions can be further refined by fine-tuning its empirical parameters. When preparing the model for fitting, its formula will be changed to the basic expression shown in equation (1), so that basic empirical parameters appear: slope  $\gamma$  and initial deviation  $K$ . Then, the model fitting process consists of modifying these two parameters to adjust the model equation.

The adjustment to the equations of the models can be achieved by finding the parameters  $E_o$  and  $\gamma$  in the equation (1). As mentioned above, the most appropriate tool to make the adjustment may be the least squares statistical method [27]. By applying this method, the following solution is obtained for the statistical estimates of the parameters  $\tilde{K}$  and  $\tilde{Y}_{SYS}$ :

$$\begin{aligned} \tilde{K} &= \frac{\sum x_i^2 \cdot \sum y_i - \sum x_i \cdot \sum x_i y_i}{n \cdot \sum x_i^2 - (\sum x_i)^2} \\ \tilde{Y}_{SYS} &= \frac{n \cdot \sum x_i y_i - \sum x_i \cdot \sum y_i}{n \cdot \sum x_i^2 - (\sum x_i)^2} \end{aligned} \quad (21)$$

Equation 21 makes possible the formal calculation of the parameters  $E_o$  and  $\gamma$  for the different models from a determined series of experimental static measurements:

$$(x_i = \log(R_i); y_i) \quad i = 1, \dots, n \quad (22)$$

By applying these deviation parameters and slope in the theoretical propagation models, a higher precision is obtained for the Okumura model since the losses calculated for the fitted model are close to the measured values. This result is shown in Fig. 9.

This means that the deviation and slope parameters of the original models can be calculated using equations (21) and

TABLE VI  
 ERROR BETWEEN PROPAGATION MODEL CALCULATIONS AND FIELD MEASUREMENTS

Model	Distance (m)	Measured Losses (dB)	Calculated Losses (dB)	Measured RSSI (dBm)	Calculated RSSI (dBm)	Error
Okumura	100	132.1	94.64	-143.1	-75.64	0.471
	200	148.1	100.66	-159.1	-81.66	0.487
	300	149.7	104.18	-160.7	-85.18	0.47
	400	148.8	106.68	-159.8	-87.68	0.451
	500	146.8	108.62	-157.8	-89.62	0.432
	600	146.8	110.2	-157.8	-91.2	0.421
	700	151.2	111.54	-162.2	-92.54	0.428
	800	147.9	112.7	-158.9	-93.7	0.413
	900	151.4	113.72	-162.4	-94.72	0.417
Hata-Cost	100	132.1	102.93	-143.1	-83.93	0.413
	200	148.1	115.86	-159.1	-96.86	0.391
	300	149.7	123.42	-160.7	-104.42	0.35
	400	148.8	128.78	-159.8	-109.78	0.312
	500	146.8	132.94	-157.8	-113.94	0.277
	600	146.8	136.34	-157.8	-117.34	0.255
	700	151.2	139.21	-162.2	-120.21	0.257
	800	147.9	141.7	-158.9	-122.7	0.231
	900	151.4	143.9	-162.4	-124.9	0.231
Longley-rice	100	132.1	78.3	-143.1	-59.3	0.586
	200	148.1	85.1	-159.1	-66.1	0.585
	300	149.7	87.8	-160.7	-68.8	0.572
	400	148.8	92.2	-159.8	-73.2	0.541
	500	146.8	99.5	-157.8	-80.5	0.49
	600	146.8	98.1	-157.8	-79.1	0.498
	700	151.2	98.7	-162.2	-79.7	0.507
	800	147.9	99.9	-158.9	-80.9	0.493
	900	151.4	99.5	-162.4	-80.5	0.505
COST 231 Walfisch Ikegami	100	132.1	90.52	-143.1	-71.52	0.5
	200	148.1	105.63	-159.1	-86.63	0.455
	300	149.7	114.47	-160.7	-95.47	0.406
	400	148.8	120.74	-159.8	-101.74	0.363
	500	146.8	125.6	-157.8	-106.6	0.324
	600	146.8	129.58	-157.8	-110.58	0.298
	700	151.2	132.94	-162.2	-113.94	0.295
	800	147.9	135.85	-158.9	-116.85	0.267
	900	151.4	138.42	-162.4	-119.42	0.265
1000	150.5	140.66	-161.5	-121.66	0.247	

(2). It is possible to further refine the accuracy of the selected model with respect to particular propagation conditions by tuning the model as described. The fitted model, whose calculations are closest to the experimental data, is Okumura (see Fig. 9), which is given by the equation (23):

$$L_{50} dB = \tilde{K} + L_F + A_{mu}(f, d) - G_{hte} - G_{AREA} - \tilde{Y}_{SYS} \quad (23)$$

Mathematically, it is given by the equation (24) that is a function of the distance ( $R$ ), frequency ( $f$ ), transmitting antenna height ( $h_{bs}$ ), receiving antenna height ( $h_{ms}$ ), and the  $\tilde{K}$  and  $\tilde{Y}_{SYS}$  calculated parameters:

$$L_{50} dB = \tilde{K} + 32.4 + 20 * \log(R) + 20 * \log(f) + 13 - 10 * \log\left(\frac{h_{bs}}{200}\right) - 10 * \log\left(\frac{h_{ms}}{3}\right) - \tilde{Y}_{SYS} \quad (24)$$

By replacing the value of  $\tilde{K}$  and  $\tilde{Y}_{SYS}$ , the equation (25) is obtained:

$$L_{50} dB = 57.34 + 32.4 + 20 * \log(R) + 20 * \log(f) + 13 - 10 * \log\left(\frac{h_{bs}}{200}\right) - 10 * \log\left(\frac{h_{ms}}{3}\right) - 15.33 \quad (25)$$

Once the adjustments are made, a comparison is made between the experimental and mathematical values found with

TABLE VII  
COMPARISON OF THE FITTED OKUMURA PROPAGATION MODEL AND  
FIELD MEASUREMENTS

Model	Distance (m)	Measured Losses (dB)	Calculated Losses with the adjusted model (dB)	Error
Okumura	100	132.10	137.90	0.044
	200	148.10	143.92	0.028
	300	149.70	147.44	0.015
	400	148.80	149.94	0.009
	500	146.80	151.88	0.034
	600	146.80	153.46	0.046
	700	151.20	154.80	0.030
	800	147.90	155.96	0.055
	900	151.40	156.98	0.036
	1000	150.50	157.90	0.048

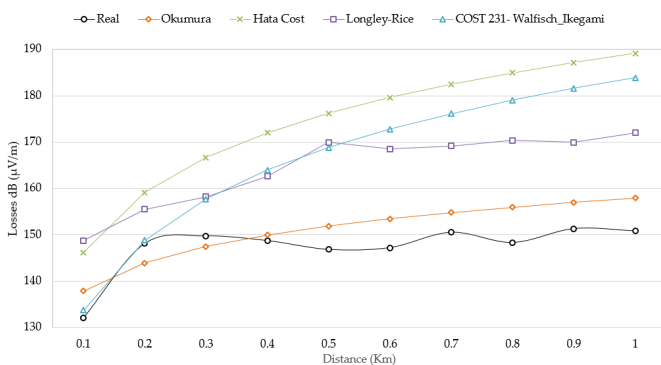


Fig. 9. Losses calculated for fitted models

equation (24), which allows determining the error that the adjusted model will have with respect to the measured field values. As can be seen in Table VII, the Okumura fitted model provides the best approximation with a mean error of 0.024 between the losses calculated with the fitted model and the measured losses.

## VII. DISCUSSION

Fig. 7 shows the theoretical propagation loss values of four propagation models with default parameters, together with experimental values. The measured path loss was greater than 53 dB above the Longley-Rice model, 40 dB above the Okumura model, 23 dB above the Walfisch-Ikegami model and 16 dB above the Hata-Cost model. This indicates that with the default parameters of the propagation models, the Hata-Cost model provides the best approximation with an average error of 0.2932 between theoretical and measured losses.

After applying equation (21), the parameters  $\tilde{K} = 57.34$  and  $\tilde{Y}_{SYS} = 15.33$  were obtained. Subsequently, the adjustment to the models was made as shown in Figure 9, from these results it is obtained that the measured path loss is approximately 40 dB below the Hata-Cost model, 25 dB below the Longley-Rice model, 6 dB below the Walfisch-Ikegami model and 5 dB above the Okumura model. Thus, the Okumura fitted model

provides the best approximation to the losses measured in the field of an urban zone of the city of Bogotá D.C., Colombia.

In this way, the proposed methodology provides an improvement to the propagation prediction model and gives criteria for the selection of the most appropriate model. So it is possible to apply the Okumura fitted in an area of unknown propagation characteristics before implementing transmitters and receivers. Theoretical results of propagation models in the tested propagation zone allow us to determine which model fits the experimental results, using the least squares criterion. These results allow us to conclude that, in a given urban area with similar geographical and urbanistic characteristics to Bogotá D.C., Colombia, the propagation of radio waves can be empirically modeled with the Okumura model given by the fitted equation (25), and the empirical parameters  $\tilde{K}$  and  $\tilde{Y}_{SYS}$  found. It is convenient to carry out this calculation of the empirically adjusted parameters in several zones, with similar propagation conditions in large and densely populated cities.

## VIII. CONCLUSION

In this work, a performance evaluation of LoRaWAN technology in a real scenario has been presented, taking into account propagation conditions in an urban environment, which are adverse for wireless transmissions and the system performance. The attained outcomes from the theoretical study have been validated by an experimental work. Coverage ranges around 1 km were attained; in turn, in an open and dense urban area. The calculation results show that the link could have a range of 1.6 to 20 km; although, RSSI measurements with the spectrum analyzer reached 1 km, while with the final device a maximum experimental transmission range of 400 m was achieved in actual transmission tests performed, a result that no model reliably predicted. Finally, with the experimental values obtained with the spectrum analyzer, sufficient data was obtained and the equations were fitted. The fitted model that had the best prediction for the proposed conditions was the Okumura model with a mean error of 0.024, which is not the best model estimated by applying the least squares criterion, although if it is the best model obtained through the fitting proposed by the ITU.

## ACKNOWLEDGMENT

The authors of the article thank the Catholic University of Colombia and its directors for the support in terms of physical, financial and human resources that were required.

## REFERENCES

- [1] A. Grunwald, M. Schaarschmidt, and C. Westerkamp, "Lorawan in a rural context: Use cases and opportunities for agricultural businesses," in *Mobile Communication - Technologies and Applications; 24. ITG-Symposium*, 2019, pp. 1–6.
- [2] J. Shenoy and Y. Pingle, "Iot in agriculture," *2016 3rd International Conference on Computing for Sustainable Global Development (INDIACom)*, pp. 1456–1458, 2016.
- [3] E. Harinda, S. Hosseinzadeh, H. Larijani, and R. M. Gibson, "Comparative performance analysis of empirical propagation models for lorawan 868mhz in an urban scenario," in *2019 IEEE 5th World Forum on Internet of Things (WF-IoT)*, 2019, pp. 154–159. [Online]. Available: <https://doi.org/10.1109/WF-IoT.2019.8767245>

- [4] J. Petäjäjarvi, K. Mikhaylov, A. Roivainen, T. Hanninen, and M. Pettissalo, "On the coverage of lpwans: range evaluation and channel attenuation model for lora technology," in *2015 14th International Conference on ITS Telecommunications (ITST)*, 2015, pp. 55–59. [Online]. Available: <https://doi.org/10.1109/ITST.2015.7377400>
- [5] J. Petäjäjarvi, K. Mikhaylov, M. Pettissalo, J. Janhunen, and J. Iinatti, "Performance of a low-power wide-area network based on lora technology: Doppler robustness, scalability, and coverage," *International Journal of Distributed Sensor Networks*, vol. 13, no. 3, p. 1550147717699412, 2017. [Online]. Available: <https://doi.org/10.1177/1550147717699412>
- [6] R. Sanchez-Iborra, J. Sanchez-Gomez, J. Ballesta-Viñas, M.-D. Cano, and A. F. Skarmeta, "Performance evaluation of lora considering scenario conditions," *Sensors*, vol. 18, no. 3, 2018. [Online]. Available: <https://www.mdpi.com/1424-8220/18/3/772>
- [7] Y. Bagariang, M. I. Nashiruddin, and N. Mufti Adriansyah, "Lora-based iot network planning for advanced metering infrastructure in urban, suburban and rural scenario," in *2019 International Seminar on Research of Information Technology and Intelligent Systems (ISRITI)*, 2019, pp. 188–193. [Online]. Available: <https://doi.org/10.1109/ISRITI48646.2019.9034583>
- [8] W. Ingabire, H. Larijani, and R. M. Gibson, "Performance evaluation of propagation models for lorawan in an urban environment," in *2020 International Conference on Electrical, Communication, and Computer Engineering (ICECCE)*, 2020, pp. 1–6. [Online]. Available: <https://doi.org/10.1109/ICECCE49384.2020.9179234>
- [9] S. Hosseinzadeh, H. Larijani, K. Curtis, and A. Wixted, "An adaptive neuro-fuzzy propagation model for lorawan," *Applied System Innovation*, vol. 2, p. 10, 03 2019. [Online]. Available: <https://doi.org/10.3390/asi2010010>
- [10] C. Ndukwe, M. T. Iqbal, and J. Khan, "Development of a low-cost lora based scada system for monitoring and supervisory control of small renewable energy generation systems," in *2020 11th IEEE Annual Information Technology, Electronics and Mobile Communication Conference (IEMCON)*, 2020, pp. 0479–0484. [Online]. Available: <https://doi.org/10.1109/IEMCON51383.2020.9284933>
- [11] D. Dobrilović, M. Malić, D. Malić, and S. Sladojevic, "Analyses and optimization of lee propagation model for lora 868 mhz network deployments in urban areas," *Journal of Engineering Management*, vol. 7, pp. 55–62, 2017.
- [12] R. El Chall, S. Lahoud, and M. El Helou, "Lorawan network: Radio propagation models and performance evaluation in various environments in lebanon," *IEEE Internet of Things Journal*, vol. 6, no. 2, pp. 2366–2378, 2019. [Online]. Available: <https://doi.org/10.1109/JIOT.2019.2906838>
- [13] A. Gehani, S. Harsha Shatagopam, R. Raghav, M. Sarkar, and C. Paolini, "Application of 915 mhz band lora for agro-informatics," in *2021 Wireless Telecommunications Symposium (WTS)*, 2021, pp. 1–4. [Online]. Available: <https://doi.org/10.1109/WTS51064.2021.9433712>
- [14] J. Michaelis, A. Morelli, A. Raglin, D. James, and N. Suri, "Leveraging lorawan to support iobt in urban environments," in *2019 IEEE 5th World Forum on Internet of Things (WF-IoT)*, 2019, pp. 207–212. [Online]. Available: <https://doi.org/10.1109/WF-IoT.2019.8767294>
- [15] A. Augustin, J. Yi, T. Clausen, and W. M. Townsley, "A study of lora: Long range & low power networks for the internet of things," *Sensors*, vol. 16, no. 9, 2016. [Online]. Available: <https://www.mdpi.com/1424-8220/16/9/1466>
- [16] A. J. Wixted, P. Kinnaird, H. Larijani, A. Tait, A. Ahmadinia, and N. Strachan, "Evaluation of lora and lorawan for wireless sensor networks," in *2016 IEEE SENSORS*, 2016, pp. 1–3. [Online]. Available: <https://doi.org/10.1109/ICSENS.2016.7808712>
- [17] P. J. Radcliffe, K. G. Chavez, P. Beckett, J. Spangaro, and C. Jakob, "Usability of lorawan technology in a central business district," in *2017 IEEE 85th Vehicular Technology Conference (VTC Spring)*, 2017, pp. 1–5. [Online]. Available: <https://doi.org/10.1109/VTCspring.2017.8108675>
- [18] A. Alsohaily, E. Sousa, A. J. Tenenbaum, and I. Maljevic, "Lorawan radio interface analysis for north american frequency band operation," in *2017 IEEE 28th Annual International Symposium on Personal, Indoor, and Mobile Radio Communications (PIMRC)*, 2017, pp. 1–6. [Online]. Available: <https://doi.org/10.1109/PIMRC.2017.8292414>
- [19] U. Alset, A. Kulkarni, and H. Mehta, "Performance analysis of various lorawan frequencies for optimal data transmission of water quality parameter measurement," in *2020 11th International Conference on Computing, Communication and Networking Technologies (ICCCNT)*, 2020, pp. 1–6. [Online]. Available: <https://doi.org/10.1109/ICCCNT49239.2020.9225615>
- [20] P. J. Marcellis, V. S. Rao, and R. V. Prasad, "Dare: Data recovery through application layer coding for lorawan," in *2017 IEEE/ACM Second International Conference on Internet-of-Things Design and Implementation (IoTDI)*, 2017, pp. 97–108.
- [21] A. M. Yousuf, E. M. Rochester, and M. Ghaderi, "A low-cost lorawan testbed for iot: Implementation and measurements," in *2018 IEEE 4th World Forum on Internet of Things (WF-IoT)*, 2018, pp. 361–366. [Online]. Available: <https://doi.org/10.1109/WF-IoT.2018.8355180>
- [22] A. I. Petrariu, A. Lavric, and E. Coca, "Lorawan gateway: Design, implementation and testing in real environment," in *2019 IEEE 25th International Symposium for Design and Technology in Electronic Packaging (SIITME)*, 2019, pp. 49–53. [Online]. Available: <https://doi.org/10.1109/SIITME47687.2019.8990791>
- [23] C. Paternina, R. Arnedo, J. Dominguez-Jimenez, and J. Campillo, "Lorawan network coverage testing design using open-source low-cost hardware," in *2020 IEEE ANDESCON*, 2020, pp. 1–6. [Online]. Available: <https://doi.org/10.1109/ANDESCON50619.2020.9272128>
- [24] F. Juliansyah, M. Z. S. Hadi, and M. Yuliana, "Implementation of rssi generated channel probing for air quality monitoring system based on lorawan," in *2021 International Electronics Symposium (IES)*, 2021, pp. 624–629. [Online]. Available: <https://doi.org/10.1109/IES53407.2021.9593936>
- [25] M. I. Nashiruddin and A. Hidayati, "Coverage and capacity analysis of lora wan deployment for massive iot in urban and suburban scenario," in *2019 5th International Conference on Science and Technology (ICST)*, vol. 1, 2019, pp. 1–6. [Online]. Available: <https://doi.org/10.1109/ICST47872.2019.9166450>
- [26] ITU Radiocommunication Sector, "Recommendation ITU-R P.1546-6 - Method for point-to-area predictions for terrestrial services in the frequency range 30 MHz to 4000 MHz," 2019. [Online]. Available: [https://www.itu.int/dms\\_pubrec/itu-r/rec/p/R-REC-P.1546-6-201908-I!!PDF-E.pdf](https://www.itu.int/dms_pubrec/itu-r/rec/p/R-REC-P.1546-6-201908-I!!PDF-E.pdf)
- [27] —, "Handbook on terrestrial land mobile radiowave propagation in the VHF/UHF bands," 2002. [Online]. Available: [https://www.itu.int/dms\\_pub/itu-r/opb/hdb/R-HDB-44-2002-OAS-PDF-E.pdf](https://www.itu.int/dms_pub/itu-r/opb/hdb/R-HDB-44-2002-OAS-PDF-E.pdf)
- [28] M. Hata, "Empirical formula for propagation loss in land mobile radio services," *IEEE Transactions on Vehicular Technology*, vol. 29, no. 3, pp. 317–325, 1980. [Online]. Available: <https://doi.org/10.1109/T-VT.1980.23859>
- [29] N. Belhadj, B. Oueslati, and T. Aguil, "Adjustment of cost231 walfisch-ikegami model for hspa+ in tunisian urban environments," in *2015 2nd World Symposium on Web Applications and Networking (WSWAN)*, 2015, pp. 1–6. [Online]. Available: <https://doi.org/10.1109/WSWAN.2015.7210330>
- [30] L. Schirru, M. B. Lodi, A. Fanti, and G. Mazzarella, "Improved cost 231-wi model for irregular built-up areas," in *2020 XXXIIIrd General Assembly and Scientific Symposium of the International Union of Radio Science*, 2020, pp. 1–4. [Online]. Available: <https://doi.org/10.23919/URSIGASS49373.2020.9232010>
- [31] V. S. Anusha, G. K. Nithya, and S. N. Rao, "A comprehensive survey of electromagnetic propagation models," in *2017 International Conference on Communication and Signal Processing (ICCSP)*, 2017, pp. 1457–1462. [Online]. Available: <https://doi.org/10.1109/ICCSP.2017.8286627>
- [32] A. G. Longley and P. L. Rice, "Prediction of tropospheric radio transmission loss over irregular terrain – A computer method," Institute for Telecommunication Sciences, Tech. Rep., 1968.
- [33] ITU Radiocommunication Sector, "Handbook on National Spectrum Management," 2015. [Online]. Available: [https://www.itu.int/dms\\_pub/itu-r/opb/hdb/R-HDB-21-2015-PDF-E.pdf](https://www.itu.int/dms_pub/itu-r/opb/hdb/R-HDB-21-2015-PDF-E.pdf)
- [34] LoRa Alliance Inc., "Lorawan™ 1.1 regional parameters," 2017. [Online]. Available: <https://lora-alliance.org/wp-content/uploads/2020/11/lorawan-regional-parameters-v1.lra.pdf>